Advancement of Reverse Electrowetting-on-Dielectric With Flexible Electrodes for Bias-Free Energy-Harvesting Applications

Karthik Kakaraparty, *Student Member, IEEE*, Erik A. Pineda, Russell C. Reid, and Ifana Mahbub, *Senior Member, IEEE*

***Abstract*—Energy harvesting with the utilization of the reverse electrowetting-on-dielectric (REWOD) phenomenon is a unique method of generating energy by implementing electrolyte impingement using mechanical modulation. The goal of wearable motion sensors that are self-powered has been undermined by the prior REWOD research's emphasis on planar electrodes, which are not flexible and require high-voltage bias to improve output power. In this article, REWOD-based energy harvesting is implemented using two sets of dissimilar flexible electrodes. The electron-beam physical vapor deposition (EBPVD) technique is utilized to coat materials on polyimide sheet. In the first planar REWOD experiment, mechanical energy was harvested through electrolyte impingement via 2-mm electrode displacement between the top and bottom electrodes. In a second REWOD experiment, the electrodes underwent a flexing test with electrolyte encapsulated between the electrodes. The planar experiment resulted in the maximum power density value of 0.002 μW/cm^2, and the proposed flexing REWOD test measurement with electrolyte encapsulated between both electrodes resulted in 0.05 μW/cm^2 of power density, which is ≈25 times higher than the value generated using the conventional REWOD setup.**

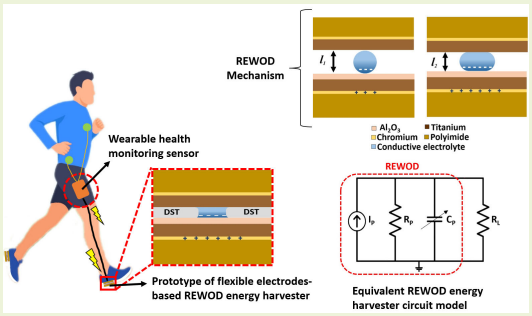

***Index Terms*— Electrolyte impingement, electromechanical modulation, energy harvesting, flexible electrodes, reverse electrowetting-on-dielectric (REWOD).**

I. Introduction

ELECTROWETTING is a long-studied phenomenon that involves a variation in the electrolyte's surface tension on the rigid surface when an electric field is applied [1], [2], [3]. Electrowetting-on-dielectric (EWOD) refers to electrowetting that occurs on a dielectrically insulated surface. The EWOD mechanism involves an applied voltage that causes a liquid droplet to move. EWOD on a highly hydrophobic surface has a wide range of applications, and Krupenkin and Taylor [4] published a paper a decade ago on the concept of electrostatic energy creation via the liquid droplet's mechanical modulation, reversing the premise of EWOD. This phenomenon, known as reverse EWOD (REWOD), makes it possible to capture energy from electrolyte impingement and has attracted the attention of numerous recent research works [5], [6], [7]. The developments in human healthcare monitoring of physical activity and illness diagnoses have greatly advanced over the last few decades [8], [9], [10], [11]. Several health habits are tracked in real time by wearable and implantable sensors, giving clinicians important data [12], [13], [14]. Wearable technology has effectively enabled continuous human health condition monitoring in routine daily activities, such as walking, running, sports, and clinical situations.

Wearable sensors have traditionally been powered by batteries, which limits the device's longevity due to the necessity for regular battery replacement, which has a direct impact on the device's performance and reliability [15], [16], [17], [18], [19]. Furthermore, batteries obstruct device downsizing

Manuscript received 10 January 2023; revised 25 February 2023; accepted 26 March 2023. Date of publication 7 April 2023; date of current version 15 May 2023. This work was supported by the National Science Foundation under Grant 2246559. The associate editor coordinating the review of this article and approving it for publication was Prof. Tao Li. *(Corresponding author: Ifana Mahbub.)*

Karthik Kakaraparty and Ifana Mahbub are with the Department of Electrical Engineering, University of Texas at Dallas, Richardson, TX 75080 USA (e-mail: Karthikeya.Kakaraparty@UTDallas.edu; ifana.mahbub@utdallas.edu).

Erik A. Pineda is with the Department of Electrical Engineering, University of North Texas, Denton, TX 76203 USA.

Russell C. Reid is with the Department of Engineering, Utah Tech University, St. George, UT 84770 USA.

Digital Object Identifier 10.1109/JSEN.2023.3264103

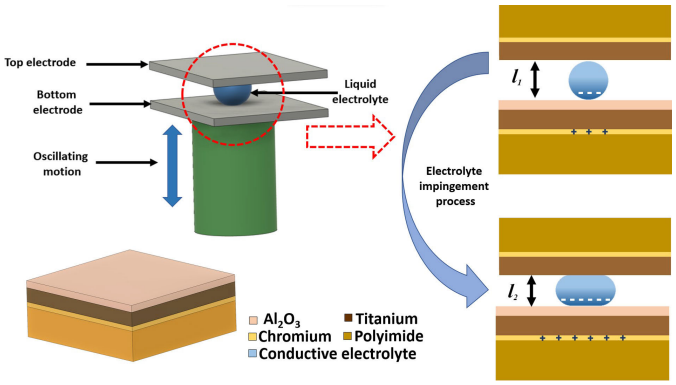

Fig. 1. Principle REWOD mechanism. The electrodes displacement owing to mechanical modulation is given by the following: $\Delta l = l_1 - l_2$.

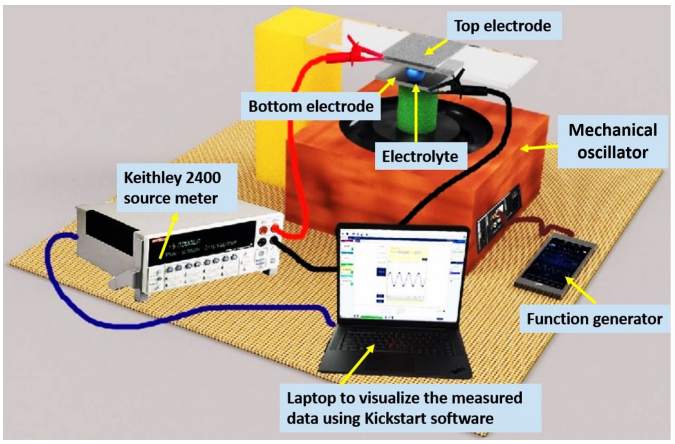

Fig. 2. Graphical visualization of the REWOD energy harvester measurement system.

and are linked to specific safety concerns, such as battery explosions and electrolyte leakage. Therefore, it is critical to develop energy harvester array that gives scope to power such sensors. Among many recently developed ambient energy-harvesting technologies, triboelectric nanogenerators (TENGs) have been shown to operate better in the lower frequency range (0.25–5 Hz), but have limitations concerning mechanical degradation. TENG's output power density and energy conversion efficiency can be significantly increased by utilizing a transistor-inspired design that can be implemented in different interfaces. Also, the design resiliency is improved, and the spatial restriction is relaxed by integrating several power generation units with a two-drain electrode architecture and a single energy collector [20], [21]. Despite significant advancements in other energy-harvesting techniques, the majority of harvesters fail to achieve high-power conversion efficiency at low frequencies with a low range of displacements (1–3 mm) [22], [23], [24].

Furthermore, the piezoelectric energy-harvesting approach necessitates continual material strain on electrodes, resulting in material degradation, which has a direct impact on the energy harvester's lifetime and reliability. Piezoelectric energy harvesters have been employed as a stable source of energy in a wide range of applications [25], [26], [27], [28]. Nevertheless, their maximum performance occurs at frequencies that are substantially higher than the typical human motion frequency range; hence, they are not suitable for self-powered human motion sensors (e.g., 1–5 Hz) [29], [30], [31]. Due to radiation damage, electromagnetic energy harvesters are not the best choice for powering wearable sensors in applications for human health monitoring. The electromagnetic device radiation is limited to 1.6 W/kg as per Federal Communications Commission (FCC) standards to reduce the amount of energy absorbed by humans and address any safety concerns. Due to the limits of current energy-harvesting technologies in terms of harvesting energy from human physical activities, a harvester device that can reliably harvest energy at a low-frequency range (less than 5 Hz) and has greater longevity is urgently needed. REWOD, a unique method of electrostatic energy harvesting, has evolved in the past decade, and there have been many research works that focused on REWOD-based energy harvesting [32], [33], [34], [35], [36]. The REWOD mechanism has been shown to work successfully at low frequencies due to its independence from solid structure resonance. REWOD involves the applied mechanical force on the electrolyte sandwiched between conductive and dielectric electrodes, resulting in the generation of a voltage owing to a variation in the electrical capacitance. As the electrolyte is continuously deformed between the aforementioned two electrodes under the application of an external mechanical force, causing a periodic change in the electrode–electrolyte interfacial area, REWOD converts the kinetic energy of liquid motion into electrical energy. Electrical double layer (EDL) and dielectric layer insulator cause capacitance at the electrolyte and electrode interface. The electrolyte impingement process is presented in Fig. 1. The mechanical modulation results in the maximum electrode displacement of Δl, which, in this work, is 2 mm, where: $\Delta l = l_1 - l_2$, in which l_1 is the maximum electrode displacement, which is 4 mm, and l_2 is the minimum electrode displacement, which is 2 mm.

The remaining sections of this article are organized as follows. The flexible electrodes fabrication and REWOD measurement setup procedure are presented in Section II. Section III presents the bending test measurements. Section IV presents the measured results of voltage, resistance, capacitance, and current generated by utilizing the fabricated flexible electrodes in the REWOD setup environment. The concluding remarks are presented in Section V.

II. Experimental Section

A. Flexible Electrode Fabrication

Polyimide sheet was utilized in the fabrication of two distinct types of electrodes. The polyimide sheet with 0.11-mm thickness is chosen, as it is flexible. A section of polyimide sheet was snipped into six identical sized portions, each having a volume of $35 \times 35 \times 0.11$ mm^3. Of these six portions, three had chromium (Cr) and titanium (Ti) coatings with the respective thicknesses of 50 and 150 nm. The remaining three samples were coated with Cr and Ti with the aforementioned thicknesses, along with a dielectric material Al_2O_3 with 100-nm thickness. The coating of the materials on the polyimide sheet has been accomplished utilizing the

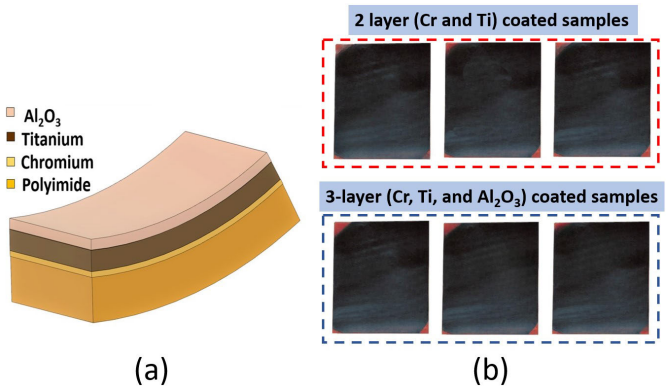

Fig. 3. Flexible three-layer-coated electrode. (a) Graphical visualization of flexible three-layer-coated electrode. (b) Fabricated electrodes.

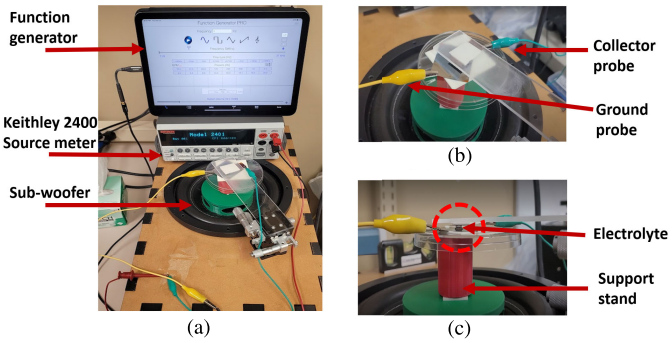

Fig. 4. (a) Measurement setup for REWOD energy harvesting. (b) Top view of the electrode–electrolyte configuration showing the collector probe and ground probe. (c) Side view portraying the electrolyte in between two flexible electrodes.

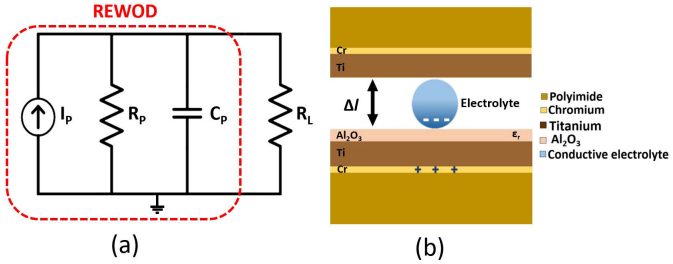

Fig. 5. REWOD energy harvester in a parallel configuration and its equivalent lumped element model. (a) Parallel configuration based REWOD equivalent lumped element model. (b) Cross-sectional view of the REWOD configuration.

electron-beam physical vapor deposition (EBPVD) method. The two-layer-coated sample is employed as the top electrode, and the previously described three-layer-coated sample served as the bottom electrode. After the completion of the coating procedure, the coating was visually examined utilizing a trinocular stereo microscope (AmScope 1140) to make sure the coating consistency.

B. Measurement Setup

The graphical visualization of the flexible REWOD energy-harvesting measurement setup is presented in Fig. 2. The electrolyte used in the experiment is a 50-μL pure deionized water that is positioned between the top and bottom flexible electrodes, with the bottom electrode supported by the stand being placed on the mechanical oscillator in order to facilitate up and down displacements, where the top electrode is having a fixed position. The fabricated electrodes are presented in Fig. 3(b). The mechanical oscillator has assigned oscillation frequency values from 1 to 5 Hz through a mobile or iPad-controlled frequency generator application. The collector probe is attached to the top electrode, and the ground probe is attached to the bottom electrode during the electrolyte impingement process to measure the ac peak-to-peak voltage recordings utilizing a Keysight oscilloscope (DS0X3014A). The other end of the collector and ground probes are connected to an impedance analyzer (AD5940) to analyze the resistance and capacitance variations due to changes in the surface area owing to the electrolyte impingement procedure.

The measurement setup for REWOD energy harvesting is presented in Fig. 4(a). The setup depicted consists of a top electrode coated with chromium (Cr) and titanium metal (Ti) layers that serve as current collectors and a bottom electrode coated with the aforementioned metal layers for electrical conduction first, followed by an Al_2O_3 metal-oxide dielectric layer. Fig. 4(b) shows the top view and Fig. 4(c) presents the side view of the electrolyte sandwiched between two electrodes. Utilizing a specially constructed subwoofer system that can be controlled by a signal-generating smartphone application (Function Generator PRO), the electrolyte positioned between the top and bottom electrodes is made to undergo an electrolyte impingement process.

The bottom electrode is attached to a support stand that is placed on the subwoofer, which oscillates up and down according to the frequency values assigned to it by the app. The frequency values range from 1 to 5 Hz with 1 Hz of step size. A signal-generating smartphone application (Function Generator PRO) app stimulates the subwoofer that enables desired amplitude displacement fluctuation along the vertical direction. The desired amplitude displacement value can be assigned manually in the app. This application works almost exactly like an actual function generator.

The REWOD configuration is theoretically understood with an electrical equivalent circuit utilizing lumped elements that are arranged in parallel, as depicted in Fig. 5(a) to the configuration presented in Fig. 5(b). The parallel configuration consists a resistor R_P, a variable capacitor C_P, variable current source I_P, and a load with resistance (R_L). The generated alternating current on the REWOD electrodes is represented by I_P, which is the rate of variation of the generated charge. Electrical resistance occurs across the electrodes as a result of the electrical conductivity, thicknesses of the electrode–electrolyte interfacial region, and the conductive layers as well as the electrolyte modulation, which causes C_P to act as a variable capacitor that varies periodically. Theoretically, as the distance between the top and the bottom electrodes decreases, the capacitance generated across both electrodes increases, and as a result, the alternating voltage and current variations can be observed, and power generated as a byproduct can be analyzed.

III. Bending Experiment for Flexible Electrodes

The fabricated three-layer (Cr, Ti, and Al_2O_3)-coated flexible electrodes underwent a flexing REWOD test to check the reliability of the three-layer coating on the polyimide substrate. The flexible electrodes were visually checked after the bending test. The coating on the polyimide sheet is intact even after the

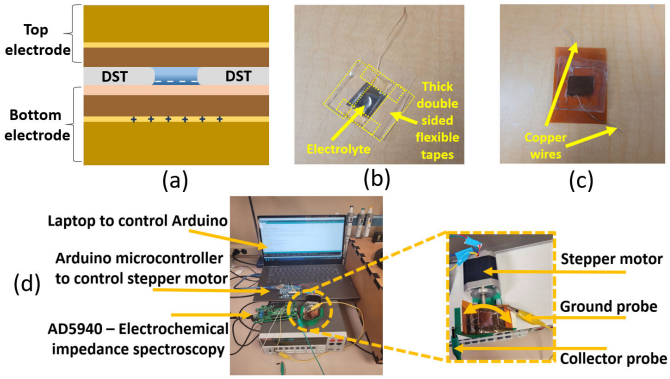

Fig. 6. Implementation of flexing REWOD test with bend-test sample. (a) Cross-sectional view of the flexing REWOD sample. (b) Electrolyte placed in the DST formed slot. (c) Enclosed structure with extended copper wires. (d) Overall test setup portraying the REWOD flexing mechanism.

samples were bent several times. A stepper motor, an Arduino microcontroller board, and a 3-D-printed model with a movable pedal were used to implement the flexing REWOD test for the fabricated flexible electrodes. The 3-D-printed model consists of a stand to hold the stepper motor and a movable pedal that is attached to the arm of the stepper motor. The flexible electrode is positioned on the fixture, and the stepper motor is controlled with an Arduino microcontroller, which is programed to rotate the stepper motor from 0° to 45° and beyond if necessary. The flexing REWOD test sample comprises top and bottom electrodes sealed together to have an electrolyte placed within the enclosed space. The top and bottom flexible electrodes were each individually connected to two copper wires that were extended outward to facilitate the connection for the measurement purpose. The copper wires enacted as collector and ground terminals for the top and bottom electrodes, respectively. The cross-sectional view of the bend-test sample is presented in Fig. 6(a). The conductive portion of the bottom electrode is connected to a copper wire, and these both are binded together by epoxy, which is cured for 24 h. The bottom electrode was surrounded by thick double-sided tape (DST), which served as a support structure to keep the electrolyte confined, as shown in Fig. 6(b). The boundary of the DST is then coated with UV-curable adhesive, and the adhesive is cured via exposure to UV light to ensure a proper seal. An electrolyte of 50 μL is used to fill the space enclosed by the DST soon after the applied glue has solidified.

The top electrode is connected with a copper wire in a manner similar to the bottom electrode. The top electrode's uncoated side is bound together utilizing a much larger DST. To complete the seal and prevent the electrolyte from leaking out, the top electrode's coated side is positioned to completely enclose the space between the two electrodes, as shown in Fig. 6(c). The bend-test sample is supported on the aforementioned 3-D-printed structure using a polyimide sheet, as shown in Fig. 6(d).

IV. Results and Discussion

A. AC Voltage Measurements

AC voltage generated utilizing the REWOD setup was measured using a Keithley 2400 Source meter and Keithley

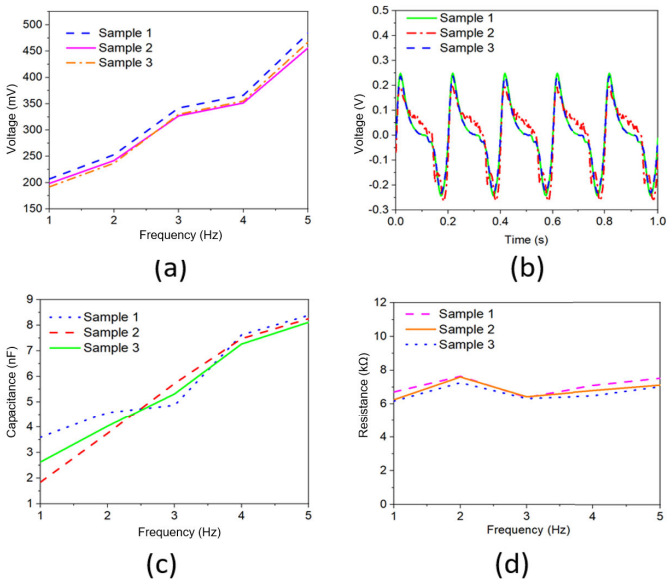

Fig. 7. (a) Voltage comparison for the considered three flexible samples. (b) Time-scale voltage plots were generated using the considered three flexible electrodes at 5-Hz modulation frequency for the first 1 s. (c) Capacitance comparison for the considered three flexible electrodes. (d) Measured resistance comparison of the three flexible electrodes.

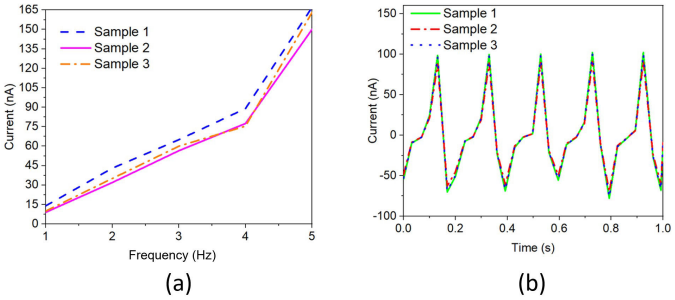

Fig. 8. (a) Current comparison for the considered three flexible samples. (b) Time-scale current plots generated using the considered three flexible samples within the first 1 s at the frequency of modulation of 5 Hz.

Kickstart 2.0 data analyzing software for a 1–5-Hz frequency range with a step size of 1 Hz. An almost linear relationship has been observed between the ac peak-to-peak voltage and the frequency. For the specified frequencies, the ac peak-to-peak voltage values were observed to be in the range of 192–484 mV. A 50-μL electrolyte with 0.33-cm^2 interfacial area between electrode and electrolyte with a 2-mm displacement variation between the electrodes was utilized to obtain these voltage ranges for all three considered flexible electrodes. The overview of voltage variations for all three samples within the 1–5-Hz frequency range is portrayed in Fig. 7(a). The peak-to-peak voltage graphs with respect to time for the first 1 s at the operating frequency of 5 Hz are presented in Fig. 7(b).

B. RC Measurements

The current source coming out of the REWOD in the modeled energy harvester is I_P, with capacitance C_P and R_P in parallel. Electrical resistance, R_P, comes to play between the electrodes because of the factors, such as the conductivity of the electrolyte, the electrolyte's thickness, conductive and dielectric layers, and the electrode–electrolyte interfacial area.

The analog front-end device AD5940 is used to measure R_P and C_P while the electrolyte impingement process. For each given frequency of oscillation, this measurement yields the system's total magnitude of impedance and phase angle

$$|Z| = \frac{1}{\sqrt{\left(\frac{1}{R_P}\right)^2 + (\omega C_p)^2}} \tag{1}$$

$$R_P = \frac{\tan(\Phi)}{\omega C_p} \tag{2}$$

$$C_P = \frac{\tan(\Phi)}{\sqrt{\left(\frac{1}{R_P}\right)^2 + (C_p\omega)^2 \times \omega \times |Z|}} \tag{3}$$

where absolute impedance is denoted by the $|Z|$, the system's resistance is R_P and capacitance is C_P, phase angle is Φ, and the ac signal's angular frequency is $\omega = 2\pi f$, in which f is the oscillation frequency. Fig. 7(c) shows a capacitance comparison for all three considered flexible electrodes/samples. Fig. 7(d) shows the measured resistance comparison of the three samples. The capacitance and resistance values for all three flexible electrodes were almost equal and followed the same trend. As the metal coating on all of the flexible electrodes used is the same, the resistance measured across those considered electrodes must be almost the same, and the RC measurements satisfied this notion.

C. AC Current Measurements

The measurement of ac current generated using REWOD setup is carried out with 1-Hz step size for a 1–5-Hz range of frequency with the help of Keithley 2400 source meter and Keithley Kickstart 2.0 data analyzing software. An increasing trend of ac current is observed with an increase in frequency with the current, and the frequency has a nearly linear relationship, as shown in Fig. 8(a). For the considered frequency range of 1–5 Hz, the ac current generated with peak-to-peak value in the range of 14–167 nA in the first trial, 9–150 nA in the second trial, and 10–163 nA in the third trial. These current ranges for all three flexible electrodes were obtained by using the same electrolyte used for obtaining voltage measurements, that is, 50-μL droplet of electrolyte (DI water) and 0.33 cm^2 of electrode–electrolyte interfacial area as mentioned earlier. The maximum measured peak-to-peak ac current at 5 Hz frequency for the first flexible electrode was 167 nA, 150 nA for the second flexible electrode, and that for the third flexible electrode was 163 nA. Fig. 8(a) shows a summary of current variations for all three flexible electrodes within the range of 1–5-Hz frequency of operation. Fig. 8(b) shows the peak-to-peak current plots with respect to time for the first 1 s at a 5-Hz operating frequency. The 484 mV of the peak voltage difference and 167 nA of peak current difference are achieved with the combination of flexible electrodes and conventional REWOD setup where the electrodes are not bent, which resulted in the generation of 0.080 μW of power. With the aforementioned electrode–electrolyte interface area, the corresponding power density value generated is estimated as 0.002 (μW/cm^2).

D. Measurement Results for the Bend Test

The flexing REWOD test produced a maximum peak-to-peak voltage of 73 mV and a maximum peak-to-peak current of 83 μA at 5-Hz operating frequency and yielding 6.059 μW of power, which may activate the ultralow-power bio-wearable chips, which typically only require power in the nanowatt range [33]. The power density generated in the flexible electrode bend test is ≈25 times higher than in the case where the flexible electrodes are not subjected to the bend test. This is due to the fact that the flexing REWOD test generated a low-resistance value of 1 kΩ at 5 Hz, which is lower than the 7-kΩ measured resistance in the case of the planar, non-bending planar REWOD structure. In addition, a 650-nF capacitance measured in the flexing REWOD test, which is ≈78 times higher than the 8.3-nF capacitance measured in the non-bending REWOD setup and is primarily responsible for the generation of higher current for the bend-test case that resulted in a higher power generation owing to the relationship, $P = V \times I$, where $V = I \times Z$. In addition, the distance between electrodes in the flexing REWOD test is approximately ranging from 0.5 to 1 mm, which is relatively four times smaller when compared with the conventional REWOD setup case, which has the electrodes distances ranging from 2 to 4 mm. This resulted in the more surface area in contact with the electrode and electrolyte in the bending experiment, as the electrolyte is enclosed within the top and bottom electrodes, which is also potentially responsible for the higher capacitance generation and, as a result, more current and, in turn, more power generation. The capacitance between electrodes is expected to increase, as the distance between them decreases, and this notion is satisfied by the corresponding R and C measurements. These aforementioned factors have justified higher power density generation in the flexing REWOD case.

The current generated out of the flexible bend test is nearly 260 times more when compared with the current generated out of the conventional REWOD setup where the samples are not bent. The high-current value generated in the bend-test case is responsible for the increased power generation in the bend-test case. At the 5-Hz frequency of operation, the time-domain voltage plot is presented in Fig. 9(a), and the time-domain current plot is presented in Fig. 9(b). The capacitance variation for the three considered bend-test trials is shown in Fig. 9(c), and Fig. 9(d) shows the measured resistance versus frequency plots for the aforementioned trials. It is observed that the magnitude of the resistance measured in the bend-test trials is less than the resistance values generated utilizing the non-bending REWOD setup. In contrast to the resistance trend, the capacitance is observed to be higher in the case of the bend test. This is due to the fact that the distance between electrodes is much less in the case of the bend test when compared with the non-bending REWOD test.

This work is compared with similar prior works considering the parameters, such as energy harvester type, the maximum frequency of operation, bias voltage, and the amount of generated power density (μW/cm^2), as shown in Table I. The frequency of operation of the proposed flexible REWOD energy-harvesting system is from 1 to 5 Hz. Even though

TABLE I
COMPARISON AMONG PRIOR WORKS

Research works	Harvester type	Single-droplet's volume (μL)	No. of droplets	Frequency [Hz]	Power-density [μW/cm^2]	Bias-voltage [V]
Adhikari *et al.* [1]	REWOD	50	1	5	3.18	No bias voltage
Krupenkin *et al.* [4]	REWOD	50	150	2	10,000	60
Yang *et al.* [6]	REWOD	50	1	3	10,960	24
Hsu *et al.* [32]	REWOD	100	16	300	10,000	4.5
Adhikari *et al.* [36]	REWOD	50	1	5	0.075	No bias voltage
Huynh *et al.* [37]	REWOD	20	1	6	0.096	1.2
This work	REWOD	50	1	5	*0.002 and **0.050	No bias voltage

*Planar REWOD setup. **Flexible REWOD setup.

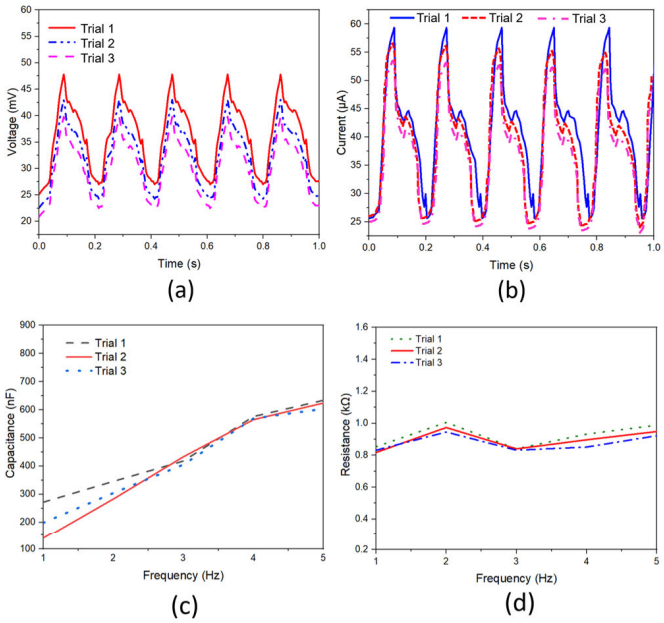

Fig. 9. Flexible REWOD bend-test results at 5-Hz frequency of modulation for three trials. (a) Time-domain voltage plots. (b) Time-domain current plots. (c) Capacitance comparison for the considered three trials. (d) Measured resistance comparison of the considered three trials.

Yang et al. [6] and Krupenkin and Taylor [4] have demonstrated ultrahigh-power density generated out of their energy-harvesting system, wherein a relatively high bias voltage has been used in prior works that helped to achieve the ultrahigh-power density. In [1], rigid rough electrodes were utilized in the REWOD energy-harvesting procedure, even though a power density of 3.18 (μW/cm^2) is demonstrated; the drawback here is that, in reality, due to structural limitations of the rigid electrodes, they are not suitable to scale up the research further for the implementation of human-locomotion-based energy harvesting. It is essential to utilize flexible electrodes to give scope for future research on bias-free REWOD energy harvesting. The polydimethylsiloxane (PDMS) substrate demonstrated in the prior work [36] is observed to be flexible but not thermally stable when compared with the polyimide substrate utilized in this work. In addition, the PDMS substrate utilized earlier resulted in slight coating inconstancy with the EBPVD procedure.

Huynh et al. [37] have used a bias voltage of 1.2 V to generate a power density value of 0.096 μW/cm^2. Whereas in our work, without using any bias voltage, utilizing a 0.33 cm^2 of electrode–electrolyte interface area, a power density value of 0.002 μW/cm^2 is generated for the REWOD system with 5-Hz frequency and 2-mm displacement. The flexing REWOD test with flexible electrodes having a 60° of bend angle has generated 73 mV of voltage and 83 μA, resulting in 6.059 μW of power, which is a relatively high amount without the utilization of bias voltage. With ≈1.2 cm^2 of electrode–electrolyte interface area, the power density value is estimated to be 0.05 μW/cm^2. In our prior work [36], PDMS flexible substrate is utilized, and the metal and metal-oxide coating procedure involved EBPVD. Whereas in this work, a polyimide flexible substrate (Kapton) is utilized with the EBPVD procedure. Also, with the visual inspection utilizing a trinocular stereo microscope (AmScope 1140), it is observed that the coating on the polyimide substrate is more consistent when compared with the 3-D-printed carbon-nanotube composite-based PDMS in [36]. It is also understood that the polyimide is preferable over the PDMS, as polyimide is more thermally stable at typical high temperatures (> 200 °C) that involve the EBPVD deposition procedure. In addition, the REWOD harvesters were not flexed; rather, they were only tested in a planar configuration. Also, [36] involved an additional step of additive manufacturing-based 3-D ink printing, whereas, in this work, this procedure is not involved making the whole process simple and time-efficient.

The REWOD measurement setup does not involve any electrical circuitry that is directly connected to data acquisition probes. The measured ac voltage and ac current data are corresponding to the electrolyte impingement mechanism to which no additional bias circuitry is connected. Also, the Keithley Series-2400 Measure Unit (SMU) offers four-quadrant precision voltage and current measurements and has noise filters within to provide low noise and high precision, and this could be the reason that no significant electrical noises were detected in the measurement results, as shown in Figs. 7(b), 8(b), and 9(a), and 9(b).

V. CONCLUSION

In this study, two dissimilar electrodes are used to accomplish REWOD-based energy harvesting. The flexible electrodes-based REWOD energy harvesting is implemented, and the voltage and current values generated using these

flexible electrodes suggested that there is a great scope for energy harvesting based on flexible electrodes. The proposed flexing REWOD test measurement with electrolyte encapsulated between both electrodes resulted in 0.05 μW/cm^2 of power density, which is $\approx$25 times higher than the value generated by modulating the REWOD without bending it. These experiments demonstrated that the flexible REWOD electrodes will be, in the future, capable to contribute to human-locomotion-based energy harvesting independent of additional bias voltage. In summary, the work presented in this article is an initial milestone for the characterization of the arrays of REWOD. For the preliminary demonstration purpose, we have evaluated a single flexing REWOD sample. As a future work, we plan to develop an array of electrolyte-enclosed structures that will involve multiple drops of electrolytes, which would increase the electrolyte–electrode interfacial area, and thus more capacitance is expected at the electrolyte–electrode interface. As a result, increased voltage and current values are expected to be generated for higher energy output and conversion efficiency.

REFERENCES

[1] P. R. Adhikari, A. B. Patwary, K. Kakaraparty, A. Gunti, R. C. Reid, and I. Mahbub, "Advancing reverse electrowetting-on-dielectric from planar to rough surface electrodes for high power density energy harvesting," *Energy Technol.*, vol. 10, no. 3, Mar. 2022, Art. no. 2100867.

[2] K. Xiao and C.-X. Wu, "Dynamics of droplets driven by electrowetting," 2022, *arXiv:2203.12391*.

[3] K. Kakaraparty, G. S. Hyer, E. A. Pineda, R. C. Reid, and I. Mahbub, "Theoretical modeling and experimental validation of reverse electrowetting on dielectric (REWOD) through flexible electrodes for self-powered sensor applications," in *Proc. IEEE Sensors*, Nov. 2022, pp. 1–4.

[4] T. Krupenkin and J. A. Taylor, "Reverse electrowetting as a new approach to high-power energy harvesting," *Nature Commun.*, vol. 2, no. 1, p. 448, Aug. 2011. [Online]. Available: https://nature.com/articles/ncomms1454

[5] P. R. Adhikari, N. T. Tasneem, R. C. Reid, and I. Mahbub, "Electrode and electrolyte configurations for low frequency motion energy harvesting based on reverse electrowetting," *Sci. Rep.*, vol. 11, no. 1, pp. 1–13, Mar. 2021.

[6] H. Yang, S. Hong, B. Koo, D. Lee, and Y.-B. Kim, "High-performance reverse electrowetting energy harvesting using atomic-layer-deposited dielectric film," *Nano Energy*, vol. 31, pp. 450–455, Jan. 2017.

[7] H. Yang, H. Lee, Y. Lim, M. Christy, and Y.-B. Kim, "Laminated structure of Al_2O_3 and TiO_2 for enhancing performance of reverse electrowetting-on-dielectric energy harvesting," *Int. J. Precis. Eng. Manuf.-Green Technol.*, vol. 8, no. 1, pp. 103–111, Jan. 2021.

[8] N. Wuthibenjaphonchai, M. Haruta, K. Sasagawa, T. Tokuda, S. Carrara, and J. Ohta, "Wearable and battery-free health-monitoring devices with optical power transfer," *IEEE Sensors J.*, vol. 21, no. 7, pp. 9402–9412, Apr. 2021.

[9] H. Dsouza, J. Pastrana, J. Figueroa, I. Gonzalez-Afanador, B. M. Davila-Montero, and N. Sepúlveda, "Flexible, self-powered sensors for estimating human head kinematics relevant to concussions," *Sci. Rep.*, vol. 12, no. 1, pp. 1–8, Jun. 2022.

[10] N. T. Tasneem, D. K. Biswas, P. R. Adhikari, R. Reid, and I. Mahbub, "Design of a reverse-electrowetting transducer based wireless self-powered motion sensor," in *Proc. IEEE Int. Symp. Circuits Syst. (ISCAS)*, Oct. 2020, pp. 1–5.

[11] S. C. Mukhopadhyay, "Wearable sensors for human activity monitoring: A review," *IEEE Sensors J.*, vol. 15, no. 3, pp. 1321–1330, Mar. 2015.

[12] X. Zeng, R. Peng, Z. Fan, and Y. Lin, "Self-powered and wearable biosensors for healthcare," *Mater. Today Energy*, vol. 23, Jan. 2022, Art. no. 100900.

[13] H. Zhang et al., "Graphene-enabled wearable sensors for healthcare monitoring," *Biosensors Bioelectron.*, vol. 197, Feb. 2022, Art. no. 113777.

[14] X. Huang et al., "Epidermal self-powered sweat sensors for glucose and lactate monitoring," *Bio-Des. Manuf.*, vol. 5, no. 1, pp. 201–209, Jan. 2022.

[15] M. A. Mohammed, F. F. Mustafa, and F. I. Mustafa, "Feasibility study for using harvesting kinetic energy footstep in interior space," in *Proc. 11th Int. Renew. Energy Congr. (IREC)*, Oct. 2020, pp. 1–4.

[16] M. Ferrari, V. Ferrari, D. Marioli, and A. Taroni, "Modeling, fabrication and performance measurements of a piezoelectric energy converter for power harvesting in autonomous microsystems," *IEEE Trans. Instrum. Meas.*, vol. 55, no. 6, pp. 2096–2101, Dec. 2006.

[17] D. J. Apo, M. Sanghadasa, and S. Priya, "Low frequency arc-based MEMS structures for vibration energy harvesting," in *Proc. 8th Annu. IEEE Int. Conf. Nano/Micro Eng. Mol. Syst.*, Apr. 2013, pp. 615–618.

[18] A. Quattrocchi, F. Freni, and R. Montanini, "Power conversion efficiency of cantilever-type vibration energy harvesters based on piezoceramic films," *IEEE Trans. Instrum. Meas.*, vol. 70, pp. 1–9, 2021.

[19] T. Ruan, Z. J. Chew, and M. Zhu, "Energy-aware approaches for energy harvesting powered wireless sensor nodes," *IEEE Sensors J.*, vol. 17, no. 7, pp. 2165–2173, Apr. 2017.

[20] W. Xu et al., "A droplet-based electricity generator with high instantaneous power density," *Nature*, vol. 578, no. 7795, pp. 392–396, Feb. 2020.

[21] H. Zheng et al., "Remote-controlled droplet chains-based electricity generators," *Adv. Energy Mater.*, vol. 13, no. 10, Mar. 2023, Art. no. 2203825.

[22] B. Andò, S. Baglio, V. Marletta, and A. R. Bulsara, "Modeling a nonlinear harvester for low energy vibrations," *IEEE Trans. Instrum. Meas.*, vol. 68, no. 5, pp. 1619–1627, May 2019.

[23] J. J. L. Aranda, S. Bader, and B. Oelmann, "An apparatus for the performance estimation of pressure fluctuation energy harvesters," *IEEE Trans. Instrum. Meas.*, vol. 67, no. 11, pp. 2705–2713, Nov. 2018.

[24] S. Hu et al., "A stretchable multimode triboelectric nanogenerator for energy harvesting and self-powered sensing," *Adv. Mater. Technol.*, vol. 7, no. 3, 2022, Art. no. 2100870.

[25] A. Roy et al., "A 6.45 μW self-powered SoC with integrated energy-harvesting power management and ULP asymmetric radios for portable biomedical systems," *IEEE Trans. Biomed. Circuits Syst.*, vol. 9, no. 6, pp. 862–874, Dec. 2015.

[26] E. Shahhaidar, O. Boric-Lubecke, R. Ghorbani, and M. Wolfe, "Electromagnetic generator: As respiratory effort energy harvester," in *Proc. IEEE Power Energy Conf. Illinois*, Feb. 2011, pp. 1–4.

[27] C. J. Lukas et al., "A 1.02 μw battery-less, continuous sensing and post-processing SiP for wearable applications," *IEEE Trans. Biomed. Circuits Syst.*, vol. 13, no. 2, pp. 271–281, Apr. 2019.

[28] C. Zhang, Y. Jin Zhou, Q. X. Xiao, L. Yang, T. Y. Pan, and H. F. Ma, "High-efficiency electromagnetic wave conversion metasurfaces for wireless energy harvesting," in *Proc. Prog. Electromagn. Res. Symp. (PIERS)*, Aug. 2016, pp. 1720–1722.

[29] S. Sankar, P.-H. Chen, and M. S. Baghini, "An efficient inductive rectifier based piezo-energy harvesting using recursive pre-charge and accumulation operation," *IEEE J. Solid-State Circuits*, vol. 57, no. 8, pp. 2404–2417, Aug. 2022.

[30] Y. C. Shu and I. C. Lien, "Analysis of power output for piezoelectric energy harvesting systems," *Smart. Mater. Struct.*, vol. 15, no. 6, pp. 1499–1512, Sep. 2006, doi: 10.1088/0964-1726/15/6/001.

[31] U. Laurentiu, C. Romeo, S. Cristina, M. Aradoaei, P. Olga, and M. Baibarac, "Flexible piezo-electric composites for 3D-printed harvesters," in *Proc. Int. Conf. Expo. Electr. Power Eng. (EPE)*, Oct. 2020, pp. 470–473.

[32] T.-H. Hsu, S. Manakasettharn, J. A. Taylor, and T. Krupenkin, "Bubbler: A novel ultra-high power density energy harvesting method based on reverse electrowetting," *Sci. Rep.*, vol. 5, no. 1, pp. 1–13, Nov. 2015.

[33] S. C. Chandrarathna and J.-W. Lee, "16.8 nW ultra-low-power energy harvester IC for tiny ingestible sensors sustained by bio-galvanic energy source," *IEEE Trans. Biomed. Circuits Syst.*, vol. 15, no. 1, pp. 55–67, Feb. 2021.

[34] P. R. Adhikari, R. C. Reid, and I. Mahbub, "High power density and bias-free reverse electrowetting energy harvesting using surface area enhanced porous electrodes," *J. Power Sources*, vol. 517, Jan. 2022, Art. no. 230726.

[35] D. Nikolov, R. Rusev, G. Angelov, and M. Spasova, "Energy harvesting system model based on reverse electrowetting," in *Proc. 26th Int. Conf. Mixed Design Integr. Circuits Syst. (MIXDES)*, Jun. 2019, pp. 302–305.

[36] P. R. Adhikari, M. N. Islam, Y. Jiang, R. C. Reid, and I. Mahbub, "Reverse electrowetting-on-dielectric energy harvesting using 3-D printed flexible electrodes for self-powered wearable sensors," *IEEE Sensors Lett.*, vol. 6, no. 5, pp. 1–4, May 2022.

[37] D. H. Huynh et al., "Environmentally friendly power generator based on moving liquid dielectric and double layer effect," *Sci. Rep.*, vol. 6, no. 1, pp. 1–10, Jun. 2016.

Karthik Kakaraparty (Student Member, IEEE) is currently a Ph.D. Candidate working under the supervision of Dr. Ifana Mahbub with the Department of Electrical and Computer Engineering, University of Texas at Dallas, Richardson, TX, USA. His current research focuses on antenna designs for applications related to millimeter wave and 5G technologies. His research interests also include REWOD energy harvesting based on flexible electrodes and antenna designs for on-body flexible electronics-based applications.

Erik A. Pineda is currently pursuing the bachelor's degree in electrical engineering with the University of North Texas, Denton, TX, USA, in Spring 2023.

He is currently with the Integrated Biomedical, RF Circuits and Systems Laboratory (iBioCASL) as a Research Assistant with software components. He enjoys working with technology, in both cases of software integration and hardware manipulation.

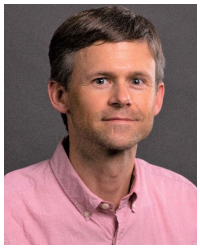

Russell C. Reid received the B.S. degree from Brigham Young University, Provo, UT, USA, in 2003, the M.E. degree from the University of Virginia, Charlottesville, VA, USA, in 2005, and the Ph.D. degree from the University of Utah, Salt Lake City, UT, USA, in 2016.

He was an Assistant Professor of Mechanical and Energy Engineering at the University of North Texas, Denton, TX, USA. He is an Assistant Professor with the Department of Engineering, Utah Tech University, St. George, UT. He has been or is currently Principle Investigator or co-PI on federally funded grants as well as internally funded university grants. He has also been heavily involved in the development of the engineering department at Utah Tech University. His research areas include energy harvesting, biosensors, and electrowetting.

Ifana Mahbub (Senior Member, IEEE) is an Assistant Professor and the Texas Instrument's Early Career Chair Awardee with the Department of Electrical and Computer Engineering, University of Texas at Dallas, Richardson, TX, USA, where she is leading the Integrated Biomedical, RF Circuits and Systems Laboratory (iBioRFCASL). She has published two book chapters, 29 journal publications, and over 62 peer-reviewed conference publications. Her research interests include energy-efficient integrated circuits and systems design for readout, wireless communication, and wireless power transfer for various implantable and wearable sensors. Her recent research interests also include ultrawideband/mm-wave phased-array antenna design for far-field wireless power transfer/vehicle to vehicle (V2V) communication for unmanned aerial vehicle (UAVs).